PROCEEDINGS OF SCIENCE

Study of the $K^{\pm} \to \pi^0\pi^0 e^{\pm}\nu$ decay with NA48/2 at CERN

Brigitte Bloch-Devaux[*†]
Department of Physics, Università degli Studi di Torino,
via P.Giuria 1, 10125 Torino, Italy
E-mail: brigitte.bloch-devaux@cern.ch

The NA48/2 collaboration has accumulated 66 000 semi-leptonic charged kaon decays $K^{\pm} \to \pi^0\pi^0 e^{\pm}\nu$, increasing the world available statistics by several orders of magnitude. Background contamination at the one percent level and very good π^0 reconstruction allow the first accurate measurement of the decay Branching Fraction and Form Factor. The achieved precision makes possible the observation of small effects such as a deficit of events at low $\pi^0\pi^0$ invariant mass which can be explained by charge exchange rescattering effects in the $\pi\pi$ system below the $2m_{\pi^+}$ threshold.

2013 Kaon Physics International Conference,
29 April-1 May 2013
University of Michigan, Ann Arbor, Michigan - USA

[*]Speaker.

[†]On behalf of the NA48/2 collaboration: G. Anzivino, R. Arcidiacono, W. Baldini, S. Balev, J.R. Batley, M. Behler, S. Bifani, C. Biino, A. Bizzeti, B. Bloch-Devaux, G. Bocquet, N. Cabibbo, M. Calvetti, N. Cartiglia, A. Ceccucci, P. Cenci, C. Cerri, C. Cheshkov, J.B. Chèze, M. Clemencic, G. Collazuol, F. Costantini, A. Cotta Ramusino, D. Coward, D. Cundy, A. Dabrowski, P. Dalpiaz, C. Damiani, M. De Beer, J. Derré, H. Dibon, L. DiLella, N. Doble, K. Eppard, V. Falaleev, R. Fantechi, M. Fidecaro, L. Fiorini, M. Fiorini, T. Fonseca Martin, P.L. Frabetti, L. Gatignon, E. Gersabeck, A. Gianoli, S. Giudici, A. Gonidec, E. Goudzovski, S. Goy Lopez, M. Holder, P. Hristov, E. Iacopini, E. Imbergamo, M. Jeitler, G. Kalmus, V. Kekelidze, K. Kleinknecht, V. Kozhuharov, W. Kubischta, G. Lamanna, C. Lazzeroni, M. Lenti, L. Litov, D. Madigozhin, A. Maier, I. Mannelli, F. Marchetto, G. Marel, M. Markytan, P. Marouelli, M. Martini, L. Masetti, E. Mazzucato, A. Michetti, I. Mikulec, N. Molokanova, E. Monnier, U. Moosbrugger, C. Morales Morales, D.J. Munday, A. Nappi, G. Neuhofer, A. Norton, M. Patel, M. Pepe, A. Peters, F. Petrucci, M.C. Petrucci, B. Peyaud, M. Piccini, G. Pierazzini, I. Polenkevich, Yu. Potrebenikov, M. Raggi, B. Renk, P. Rubin, G. Ruggiero, M. Savrié, M. Scarpa, M. Shieh, M.W. Slater, M. Sozzi, S. Stoynev, E. Swallow, M. Szleper, M. Valdata-Nappi, B. Vallage, M. Velasco, M. Veltri, S. Venditti, M. Wache, H. Wahl, A. Walker, R. Wanke, L. Widhalm, A. Winhart, R. Winston, M.D. Wood, S.A. Wotton, A. Zinchenko, M. Ziolkowski.

PoS(KAON13)028

1. Introduction

Results of a detailed study of 1.1 million $K^{\pm} \to \pi^+\pi^- e^{\pm}\nu$ decays (denoted K^{+-}_{e4}) has been reported at this conference [1], based on publications by the NA48/2 experiment [2, 3]. This study is now complemented by the analysis of a large, although smaller, sample of 66 000 $K^{\pm} \to \pi^0\pi^0 e^{\pm}\nu$ decays (denoted K^{00}_{e4}). Very limited information is available from studies of a total of 37 observed K^{00}_{e4} events in three different experiments [4, 5, 6] combined in a branching ratio value of $(2.2 \pm 0.4) \times 10^{-5}$ [7] and a constant form factor value $|V_{us}| \cdot F = 1.49 \pm 0.13$. The more recent experiment E470 at KEK [8] observed about 210 such decays from stopped kaons in an active target but this result was affected by large systematic uncertainties which hindered its gain in statistical precision.

On the theoretical side, isospin symmetry properties predict a relation between the partial rates of the K_{l4} decays in charged and neutral kaons modes: $\Gamma(K^{+-}_{l4}) = \frac{1}{2}\Gamma(K^{0\pm}_{l4}) + 2\Gamma(K^{00}_{l4})$ where $l = e, \mu$ and $K^{0\pm}_{l4}$ denotes the $K^0 \to \pi^0\pi^{\pm}l^{\mp}\nu$ decay mode. The first two partial rates are measured with $1-2\%$ relative precision while the last one is known within 18% only. Predictions have also been reported from Chiral Perturbation Theory calculations [9] using the form factor descriptions available from the first K^{+-}_{e4} experiment with sizable statistics [10]. Using the leading partial wave contribution to the decay amplitude, the branching ratio value is predicted to be $\mathrm{BR}(K^{00}_{e4}) = (2.01 \pm 0.11) \times 10^{-5}$, where the 5% relative error comes from the form factors experimental precision in [10].

Preliminary precise measurements have been obtained by the NA48/2 experiment and are reported here.

2. Beam and detector performances

The beam and experimental setup has been already described several times at this conference [11]. Full details can be found in [12]. The important detector components for this analysis are:

• a magnetic spectrometer consisting of a dipole magnet surrounded by two sets of drift chambers achieving a momentum resolution $\sigma(p)/p = (1.02 \oplus 0.044\ p)\%$ (p in GeV/c);

• a 27 radiation length liquid krypton calorimeter (LKr) measuring electromagnetic energy deposits and identifying electrons through their E/p ratio (the energy resolution achieved is $\sigma(E)/E = (3.2/\sqrt{E} \oplus 9.0/E \oplus 0.42)\%$ (E in GeV) and the space resolution for isolated showers is $\sigma_x = \sigma_y = (0.42/\sqrt{E} \oplus 0.06)$ cm);

• a two plane segmented scintillator hodoscope triggering the detector readout on charged track topologies with a time resolution of $\sim$150 ps;

• a two-level trigger logic selecting events with at least one track giving hits in the two hodoscope planes and energy deposits in the LKr calorimeter consistent with at least 2 photons, and not consistent with the decay of a 60 GeV/c kaon decay $K^{\pm} \to \pi^+\pi^0$.

3. Formalism and event selection

Four-body decays are fully described by five kinematic variables. The presence of two identical particles in the final state reduces the number of variables to three: the squared invariant masses

of the dipion $S_\pi = M^2_{\pi^0\pi^0}$ and dilepton $S_e = M^2_{e\nu}$, and the angle θ_e of the electron in the dilepton rest frame with respect to the line of flight of the dilepton in the kaon rest frame. As the dipion system can only have isospin $I = 0$ and orbital momentum $l = 0$, only one form factor (F_s) enters in the decay amplitude expression and the $\cos\theta_e$ distribution does not carry any particular information.

The K^{00}_{e4} candidates are reconstructed from one charged particle measured in the spectrometer and four photons, identified from their energy deposits in the LKr calorimeter, and forming two π^0s pointing to the same decay vertex. The kinematic separation of the signal candidates from the abundant $K^{\pm} \to \pi^0\pi^0\pi^{\pm}$ decays (denoted $K^{00}_{3\pi}$) with a similar final state topology is obtained by requiring missing mass and and missing transverse momentum in the $\pi^0\pi^0\pi^{\pm}$ decay hypothesis (Figure 1).

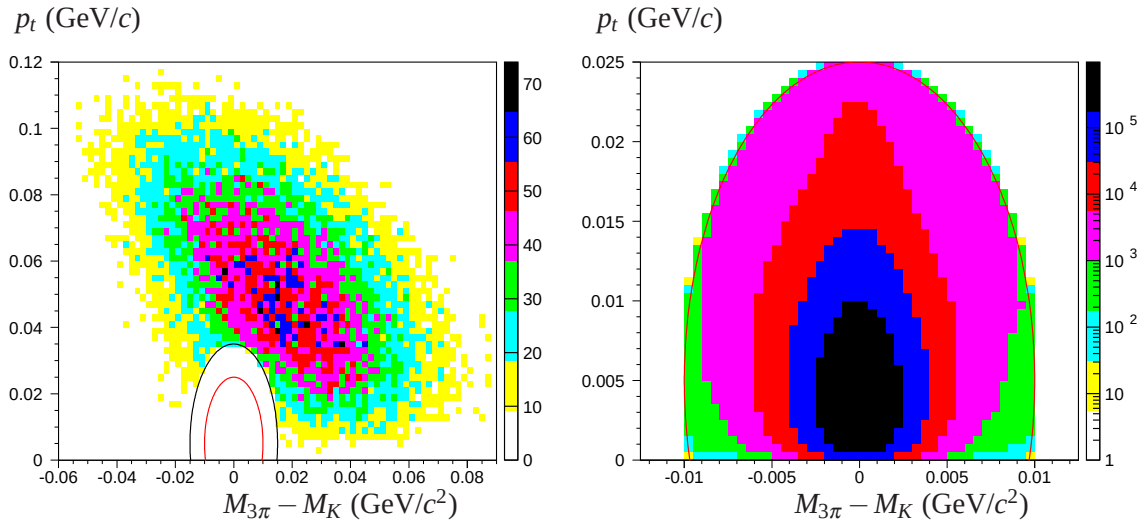

Figure 1: Reconstructed $(M_{3\pi} - M_K, p_t)$ plane for the signal K^{00}_{e4} candidates (left) and the same topology $K^{00}_{3\pi}$ candidates (right). $M_{3\pi}$ is the reconstructed three pion invariant mass and M_K the nominal kaon mass. Signal events are selected outside an ellipse centered on the nominal kaon mass and 5 MeV/c p_t, with semi-axes of 15 MeV/c^2 and 30 MeV/c^2 respectively (black contour). $K^{00}_{3\pi}$ candidates are required to be located inside an ellipse with same center but with semi-axes of 10 MeV/c^2 and 20 MeV/c^2 respectively (smaller red contour enlarged in the right plot). Note the linear color scale of the left plot and the logarithmic color scale of the right plot.

Extra requirements of electron identification are then applied:

- charged track momentum larger than 5 GeV/c;
- E/p ratio of associated energy E, measured in the LKr calorimeter, and momentum p, measured in the spectrometer, between 0.9 and 1.1;
- properties of associated LKr shower consistent with the electron hypothesis.

The background to K^{00}_{e4} candidates is threefold:

- $K^{00}_{3\pi}$ decay with the charged pion faking an electron response in the LKr calorimeter;
- $K^{00}_{3\pi}$ decay followed by $\pi^{\pm} \to e^{\pm}\nu$ decay ($\sim 8\%$ of these $\pi^{\pm}$ subsequently decay, mostly to $\mu^{\pm}\nu$ while $\mathrm{BR}(\pi e\nu) = 1.23 \times 10^{-4}$);
- accidental coincidence of another kaon decay with an additional track or photon resulting in the same final state topology as the signal.

The first and third contributions are measured from data studies while the second source,

including a genuine electron, is estimated form a dedicated simulation. The background (B) to signal (S) ratio is: B/(S+B) = 1.07% with individual contributions from the three identified sources of 0.71%, 0.12% and 0.24%, respectively.

4. Form factor measurement

The differential rate in the plane (S_π, S_e) is proportional to F_s^2. It is compared, after background subtraction, to the same distribution obtained from a simulation using a constant form factor and taking into account acceptance, resolution, trigger efficiency and radiative effects in the 2-dimensional plane. For this purpose, a detailed GEANT3-based [13] Monte Carlo simulation is used. It includes full detector geometry, material description and local detector imperfections. Radiative effects include real photon emission at the decay vertex and are simulated using the program PHOTOS [14].

The data and simulated samples are distributed over a grid of (11×10) equally populated bins in the dimensionless variables $q^2 = S_\pi/4m_{\pi^+}^2 - 1$ and $S_e/4m_{\pi^+}^2$. The first q^2 bin (below the $2m_{\pi^+}$ threshold and therefore with $q^2 < 0$ values) contains 6 000 events and is further divided into two equal population boxes. The ratio of the data and simulation distributions is displayed in Figure 2 projected on the q^2 axis and normalized to unity at $q^2 = 0$ without prior assumption of its variation which shows a cusp-like shape at the $2m_{\pi^+}$ threshold.

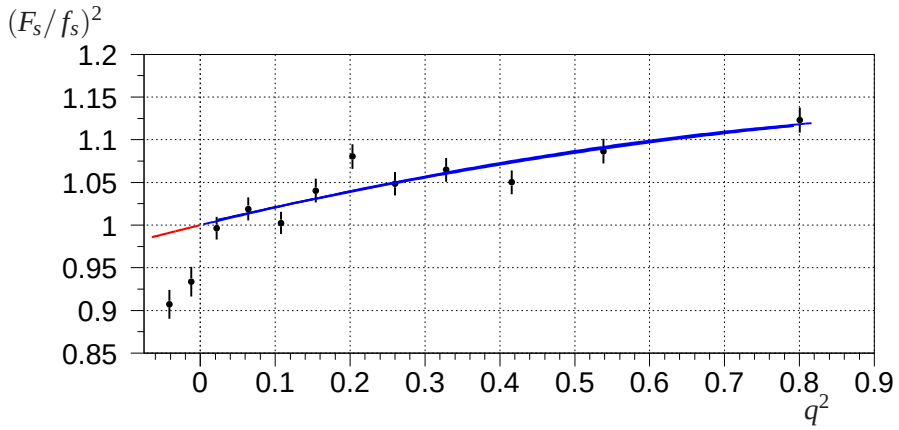

Figure 2: Ratio of Data and simulated distributions along the q^2 axis. The line is a polynomial fit to the data points with $q^2 > 0$ and is extrapolated below the threshold to emphasize the observed deficit of events. The normalization f_s is imposed by constraining the ratio to unity at threshold.

Fits are then performed in the 2-dimensional plane to determine the coefficients of a series expansion parameterization of F_s, minimizing a χ^2 estimator summed over bins with $q^2 > 0$. Two parameterizations have been considered:

$$F_s = f_s + f_s' \cdot q^2 + f_s'' \cdot q^4 \ , \tag{4.1}$$

$$F_s = f_s + f_s' \cdot q^2 + f_s'' \cdot q^4 + f_e' \cdot S_e/4m_{\pi^+}^2 \ . \tag{4.2}$$

Systematic uncertainties include possible effects from fit procedure, reconstruction, trigger efficiency corrections, acceptance, background and electron-identification control, and radiative

events modeling. Fit results are listed in Table 1 and displayed in Figure 3 together with the results obtained in the K^{+-}_{e4} analysis [2].

Table 1: Fits results in the 2-dimensional plane $(q^2, S_e/4m^2_{\pi^+})$. The improved normalized χ^2 value supports the additional F_S variation with S_e. When using (4.1), the correlation between the fit parameters is -0.954. For (4.2), the correlation between the q^2 slope and curvature is -0.946 and the correlations with the $S_e/4m^2_{\pi^+}$ slope are 0.189 and -0.063 respectively. Preliminary systematic uncertainties are quoted for the most elaborate fit.

parameterization	Eq. (4.1)	Eq. (4.2)
f'_s/f_s	$0.110 \pm 0.032_{stat}$	$0.136 \pm 0.033_{stat} \pm 0.015_{syst}$
f''_s/f_s	$-0.051 \pm 0.039_{stat}$	$-0.060 \pm 0.039_{stat} \pm 0.015_{syst}$
f'_e/f_s	–	$0.110 \pm 0.024_{stat} \pm 0.022_{syst}$
χ^2/ndf	1.22 (8% probability)	0.97 (54% probability)

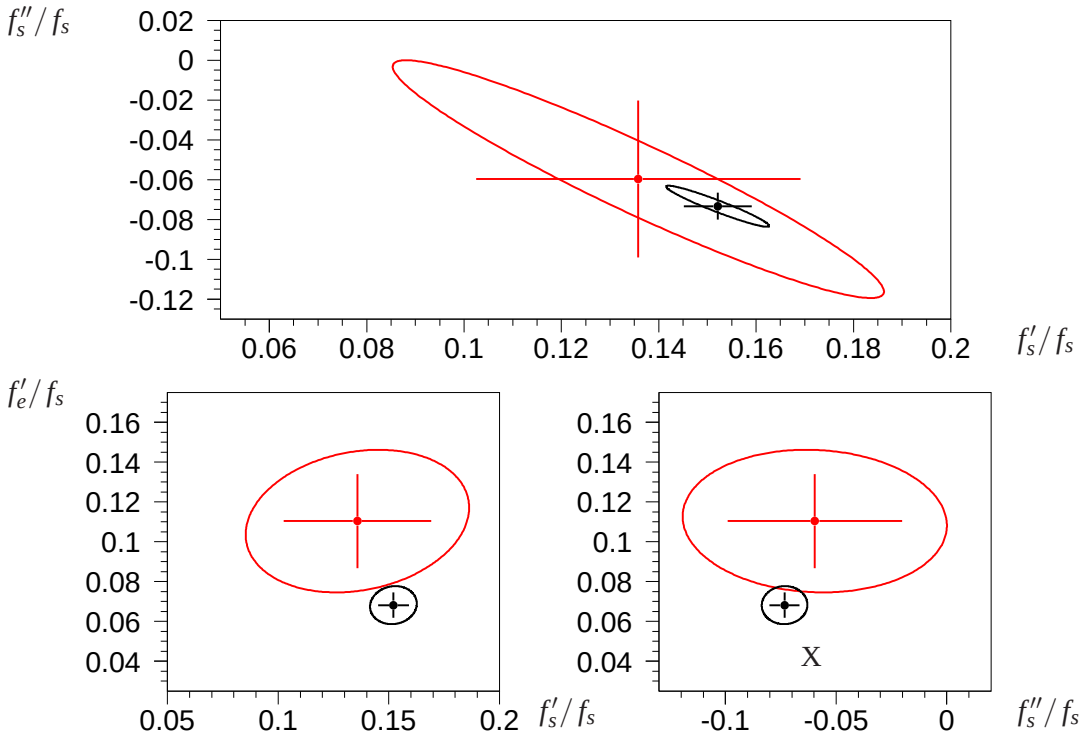

Figure 3: Form factor fitted parameters using (4.2) in the three 2-dimensional planes (red 68% CL contours). Values obtained in the K^{+-}_{e4} analysis are displayed as well (black 68% CL contours) in good agreement with the preliminary K^{00}_{e4} results. Errors are statistical only.

A possible interpretation of the cusp-like shape of the F_S^2 form factor near the $2m_{\pi^+}$ threshold is the effect of final state charge exchange scattering in the K^{+-}_{e4} mode, similarly to that observed in the $M^2_{\pi^0\pi^0}$ distribution analysis of the $K^{00}_{3\pi}$ decay [15]. The interference between the unperturbed amplitude and the scattering amplitude (imaginary above threshold, real and negative below) at one-loop [16] is sufficient to explain the shape and size of the deficit of events observed in Figure 2. Further investigations will be performed before finalizing these preliminary results.

5. Branching ratio measurement

The branching ratio is measured relative to the abundant mode $K^{00}_{3\pi}$ which presents the same topology as the K^{00}_{e4} signal mode and is recorded concurrently through the same trigger logic, minimizing systematic effects which partially cancel between signal and normalization:

$$\mathrm{BR}(K^{00}_{e4}) = \frac{N_s - N_b}{N_n} \cdot \frac{A_n\,\varepsilon_n}{A_s\,\varepsilon_s} \cdot \mathrm{BR}(n),$$

where N_s, N_b, N_n are the numbers of signal, background and normalization candidates, A_s and ε_s (A_n and ε_n) are the geometrical acceptance and trigger efficiency for the signal (normalization) sample, respectively. The normalization branching ratio $\mathrm{BR}(n) = (1.761 \pm 0.022)\%$ is the world average [7]. The normalization mode has been studied extensively by NA48/2 [15, 17]. The $K^{00}_{3\pi}$ candidates follow the signal event selection (Sec.3) apart from the kinematic cut in the plane $(M_{3\pi} - M_K, p_t)$ (Figure 1) and the electron-identification, replaced by a pion-identification (charged track momentum larger than 5 GeV/c). Acceptances are obtained from the simulation ($\sim 4\%$ for the normalization mode, $\sim 2\%$ for the signal mode) and include the detailed description of form factors as measured by NA48/2. Trigger efficiencies ε_s and ε_n are similar ($\sim 97\%$) and determined from control data samples. A total of 66 000 signal candidates, 708 background events and $94 \cdot 10^6$ normalization events are used for the branching ratio measurement. Systematic uncertainties take into account the control of acceptance, form factors description, background estimate, trigger cuts, particle identification and radiative events modeling. Simulation statistics and trigger efficiency precision are of statistical origin. The preliminary value is obtained as the combination of ten statistically independent samples (Figure 4), each collected within stable data taking conditions:

$$\mathrm{BR}(K^{00}_{e4}) = (2.585 \pm 0.010_{stat} \pm 0.010_{syst} \pm 0.032_{ext}) \times 10^{-5}, \tag{5.1}$$

where the dominating external error comes from the normalization mode branching ratio.

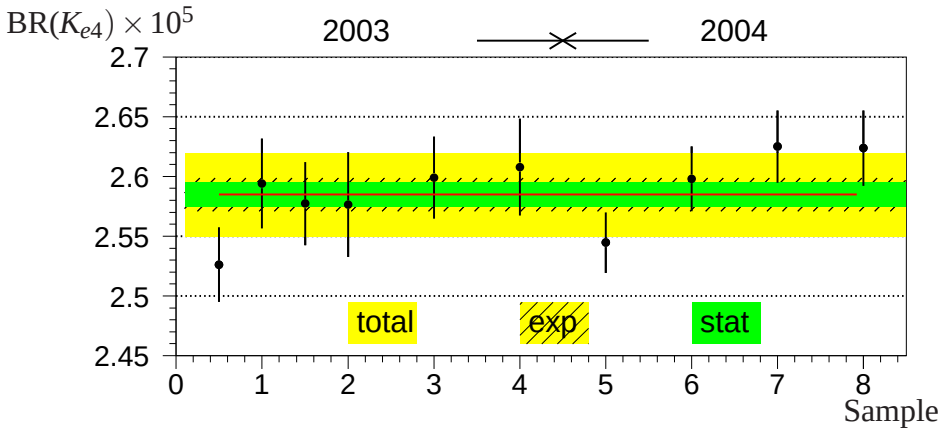

Figure 4: K_{e4} branching ratio for ten statistically independent samples each averaged over both kaon charges. The hatched band shows the experimental error ($\sigma_{exp} = \sigma_{stat} \oplus \sigma_{syst}$). The total error (shaded band) includes the external error.

The K^{00}_{e4} branching ratio, inclusive of radiative decays, can also be expressed as:

$$\mathrm{BR}(K^{00}_{e4}) = \tau_{K^{\pm}} \cdot (|V_{us}| \cdot f_s)^2 \cdot I_3, \tag{5.2}$$

where $\tau_{K^\pm}$ is the $K^\pm$ mean lifetime (in seconds) and I_3 is the integrated differential rate over the 3-dimensional space after substituting the form factor by its measured value, including radiative effects and leaving out the $|V_{us}|$ and f_s constants. The value of f_s is then obtained from the measured value of BR(K^{00}_{e4}) and the integration result. Using (5.1) and the world average kaon lifetime value $(1.2380 \pm 0.0021) \times 10^{-8}$ s, the measurement of the form factor is now complemented by its overall f_s normalization:

$$|V_{us}| \cdot f_s = 1.372 \pm 0.003_{stat} \pm 0.004_{syst} \pm 0.008_{ext},$$
$$\text{corresponding to } f_s = 6.092 \pm 0.012_{stat} \pm 0.017_{syst} \pm 0.045_{ext},$$

when using $|V_{us}| = 0.2252 \pm 0.0009$ [7]. The statistically significant difference from the f_s value obtained in the K^{+-}_{e4} mode [3] suggests to include in the form factor determination a more refined modeling of the isospin breaking effects than the naive description used here.

6. Summary and prospects

From a sample of 66 000 K^{00}_{e4} candidates with about 1% background, the NA48/2 experiment has presented preliminary values of the branching ratio and form factor at percent level precision. The observation of a cusp-like structure in the form factor variation with q^2 can be explained by final state charge exchange scattering in the corresponding K^{+-}_{e4} mode. From the same data sample, both $K^{00}_{\mu 4}$ and $K^{+-}_{\mu 4}$ modes could be observed potentially with a few thousand candidates exploring the still uncharted world of $K_{\mu 4}$ decays.

Acknowledgments

It is a pleasure to thank the local organizing committee for their warmest hospitality at Michigan University. The author is grateful for this great opportunity of enjoyable discussions with colleagues from other kaon experiments as well as theory experts.

References

[1] B. Bloch-Devaux, this conference, PoS(KAON13) **025**.

[2] NA48/2: J. Batley et al., Eur. Phys. J. **C70** (2010) 635.

[3] NA48/2: J. Batley et al., Phys. Lett. **B715** (2012) 105.

[4] D. Cline and Q. Ljung, Phys. Rev. Lett. **28** (1972) 1287.

[5] V. Bolotov et al, Sov. J. Nucl. Phys. **44** (1986) 68.

[6] V. Barmin et al, Sov. J. Nucl. Phys. **48** (1988) 1032.

[7] PDG: J. Beringer et al., Phys. Rev. **D86** (2012) 010001.

[8] E470: S. Shimizu et al, Phys. Rev. **D70** (2004) 037101.

[9] J. Bijnens, G. Colangelo, J. Gasser, Nucl. Phys. **B427** (1994) 427.

[10] S118: L. Rosselet et al., Phys. Rev. **D15** (1977) 574.

[11] Contributions to this conference, PoS(KAON13) **012, 013, 017, 025, 030**.

[12] NA48: V. Fanti et al., Nucl. Instrum. Methods **A574** (2007) 433.

[13] Geant: CERN program library long writeup **W5013** (1994).

[14] E. Barberio and Z. Was, PHOTOS, Comp. Phys. Comm. **79** (1994) 291.

[15] NA48/2: J. Batley et al., Eur. Phys. J. **C64** (2009) 589.

[16] N. Cabibbo, G. Isidori, J. High Energy Phys. **03** (2005) 021.

[17] NA48/2: J. Batley et al., Phys. Lett. **B686** (2010) 101.